

Alternative SERRS probes for the immunochemical localization of ovalbumin in paintings: an advanced mapping detection approach

Cite this: *Analyst*, 2013, **138**, 4532

Giorgia Sciutto,^a Lucio Litti,^b Cristiana Lofrumento,^{cd} Silvia Prati,^a Marilena Ricci,^{cd} Marina Gobbo,^b Aldo Roda,^e Emilio Castellucci,^{cd} Moreno Meneghetti^{*b} and Rocco Mazzeo^{*a}

In the field of analytical chemistry, many scientific efforts have been devoted to develop experimental procedures for the characterization of organic substances present in heterogeneous artwork samples, due to their challenging identification. In particular, performances of immunochemical techniques have been recently investigated, optimizing *ad hoc* systems for the identification of proteins. Among all the different immunochemical approaches, the use of metal nanoparticles – for surface enhanced Raman scattering (SERS) detection – remains one of the most powerful methods that has still not been explored enough for the analysis of artistic artefacts. For this reason, the present research work was aimed at proposing a new optimized and highly efficient indirect immunoassay for the detection of ovalbumin. In particular, the study proposed a new SERRS probe composed of gold nanoparticles (AuNPs) functionalised with Nile Blue A and produced with an excellent green and cheap alternative approach to the traditional chemical nanoparticles synthesis: the laser ablation synthesis in solution (LASIS). This procedure allows us to obtain stable nanoparticles which can be easily functionalized without any ligand exchange reaction or extensive purification procedures. Moreover, the present research work also focused on the development of a comprehensive analytical approach, based on the combination of potentialities of immunochemical methods and Raman analysis, for the simultaneous identification of the target protein and the different organic and inorganic substances present in the paint matrix. An advanced mapping detection system was proposed to achieve the exact spatial location of all the components through the creation of false colour chemical maps.

Received 8th January 2013

Accepted 10th May 2013

DOI: 10.1039/c3an00057e

www.rsc.org/analyst

Introduction

In the last few decades, many scientific efforts have been aimed at developing innovative analytical procedures for the characterization of artwork samples. Among different paint materials, organic substances – used since ancient times as binders, varnishes and adhesives – have drawn the attention of specific researchers, due to their challenging identification caused by their limited amount in samples and their noticeable ability to undergo physicochemical changes with ageing. In addition, their identification plays a crucial role in the characterization of

the execution technique, in authentication studies and in the selection of adequate methodologies for conservation and restoration purposes.

Immunochemical techniques, widely employed in bio-analytical and clinical chemistry,¹ were proposed some years ago^{2,3} in the field of Cultural Heritage. Recently, their performances have been deeply investigated, optimizing *ad hoc* systems for the identification of different protein types within multilayered and complex matrices, such as paint stratigraphies. These methodologies exploited the high selectivity of antigen–antibody reactions, which allows discrimination of different proteins and to determine their biological source. Different markers and detection techniques have been combined for the visualization of antigen–antibody complexes, using enzymes,^{4,5} fluorochromes^{6,7} and gold nano-particles⁸ as markers for sensitive localization of proteins within paint cross-sections. Nevertheless, immuno-based methods, which employ detection systems such as chemiluminescence or fluorescence, are not able to provide information on different organic and inorganic substances, which constitute (alone or in mixtures) the paint layers. This may compromise a thorough characterization of the artworks and

^aMicrochemistry and Microscopy Art Diagnostic Laboratory, University of Bologna, Via Guaccimanni 42, 48121 Ravenna, Italy. E-mail: rocco.mazzeo@unibo.it; Fax: +39 0544 937159; Tel: +39 0544 937150

^bDepartment of Chemical Sciences, University of Padova, Via Marzolo, 1, 35131 Padova, Italy. E-mail: moreno.meneghetti@unipd.it; Tel: +39 0498275127

^cDepartment of Chemistry, Polo Scientifico e Tecnologico, University of Firenze, Via della Lastruccia 3, 50019 Sesto Fiorentino Firenze, Italy

^dLENS, Polo Scientifico e Tecnologico, University of Firenze, Via N. Carrara 1, 50019 Sesto Fiorentino Firenze, Italy

^eDepartment of Chemistry "G. Ciamician", University of Bologna, 40126 Bologna, Italy

studies required for restoration and attribution purposes. Moreover, it is worth mentioning that, due to the uniqueness and rarity of specimens, maximum information should be achieved from a minimum number of samples, meaning that a single type of analysis should provide information on different types of materials. For this reason, among all the different immunochemical approaches, Raman microscopy may be one of the most powerful methods, still not explored enough. Such an approach is based on the combination of the traditional spectroscopic characterization of paint layers (which provides molecular information on Raman active compounds) with the selective identification of a target protein employing immuno-based surface enhanced Raman scattering (SERS) detection.

Enhancement of the Raman signal, which has a very low scattering cross-section with respect to fluorescence, can be ascribed to an electromagnetic enhancement mechanism related to the amplification of incident light fields by a localized surface plasmon resonance. This mechanism allows the detection of Raman-active molecules (Raman reporters) adsorbed on the surface of metallic nanostructures. The maximum SERS enhancement occurs in specific regions of the nanoparticles' surface, the so-called hot-spots. In this particular condition Raman scattering may increase by more than 10–12 orders of magnitude in cases of single-molecule vibrational studies. The average enhancement factor, ranging between 3 and 7 orders of magnitude,^{9–12} allows, in any case, a very good sensitivity for analyte recognition. Hot spots are local areas with a very strong electromagnetic enhancement and many times they can be identified as junctions or close interactions between plasmonic objects,¹² which can be easily obtained with the aggregation of nanoparticles. In fact, among such nano-structures, where the distances can be of the order of 1 nm or less, very high enhancements can be obtained by exciting their localized surface plasmons.^{13,14}

Moreover, Raman signals can also be improved through the surface enhanced resonant Raman scattering (SERRS) effect, which occurs when a Raman reporter is in resonance with the laser excitation wavelength.¹⁵

In the last few decades, the evident potentialities of such systems allowed the introduction of SERS probes – which consist of plasmonic nanoparticles with a Raman reporter anchored to their surface – in immunochemical approaches applied in biomolecules' detection in physiological and pathological processes in cells and tissues.^{16–19}

However, even if the application of both SERS and SERRS techniques is not new in the field of Cultural Heritage (*e.g.* for the determination of very low concentrations of organic pigments or colorants^{20–24}) to the authors' knowledge, only one research study on the combination of SERS analysis and immunological methods was reported in the literature.⁸ In that study, several drawbacks of the proposed assay were cited and ascribed to the non-specific immuno-SERS signals, arising from the paint matrix. In more detail, difficulties in removing the excess of SERS nanotag complexes were declared, either in the presence or absence of the primary antibody. The authors connected this experimental evidence to the use of a feeble blocking agent and treatment, in an attempt to not affect the

weak positive SERS signal, which can be seriously compromised. In addition, the potentialities of the combined approach with the traditional Raman microscopy for the simultaneous localization of Raman active compounds present in the paint matrix are not evaluated, opening the way for substantial improvement.

Within this scenario, the present research work was aimed at proposing a new optimized and highly efficient indirect immunoassay, based on the use of alternative SERS labels for the selective localisation of ovalbumin in paint cross-sections. In particular, gold nanoparticles (AuNPs) employed for the creation of SERS-nanotags were obtained with laser ablation synthesis in solution (LASiS).

LASiS allows us to obtain stable nanoparticles which are charged and for this reason no stabilizing molecules are needed. Consequently, these gold particles can be easily functionalized without any ligand exchange reaction or extensive purification procedures, also reducing the formation of chemical waste.²⁵

In addition, aggregated AuNPs, with a large number of “hot spots”, are obtained by means of a physical method such as an optimized centrifugation procedure. The aggregated nanostructures were also coated with polyethylene glycol (PEG), in order to minimize the non-specific signals arising from the sample matrices. The potentialities of such a system, functionalized with SERS reporters and antibodies, have been recently described in developing plasmonic nanostructures for ultrasensitive multiplexed identification of tumor-associated antigens.²⁶

The present work was aimed at developing a comprehensive analytical approach for the investigation of paint cross-sections, based on the combination of immune-SERS and Raman analysis, using new SERS nanotags obtained with LASiS.

In particular, Nile Blue A functionalized with lipolic acid (LipNB)²⁷ to promote the linking to gold nanoparticles was used as the SERS reporter. The high efficiency of Nile Blue A as a Raman active molecule with 633 nm laser excitation has already been investigated¹⁵ while, in the present research, its versatility to be detected with the 785 nm laser excitation is also demonstrated. The peculiar spectral features of this molecule, which are well differentiated from those of other components of a paint stratigraphy, allow production of an unambiguous positive signal and highly sensitive identification of immuno-complexes.

Indeed, an advanced mapping system was proposed to determine the exact spatial location of all the components through the creation of false colour chemical maps.

The methodology was optimized and evaluated on standard samples prepared in the laboratory – presenting different paint structures and compositions – and on a historical sample collected from a Renaissance panel painting.

Experimental

Reagents and materials

Anti-chicken egg albumin antibody (whole antiserum, produced in rabbit) and the blocking agent bovine non-fat dried milk were purchased from Sigma-Aldrich (St Louis, MO, USA). Polyclonal

anti-rabbit IgG antibody (produced in goat) was purchased from AbCam (Cambridge, UK).

Nile Blue A perchlorate, lipoic acid, 1-[bis(dimethylamino)methylene]-1*H*-1,2,3-triazolo[4,5-*b*]pyridinium 3-oxide hexafluorophosphate (HATU), 2,4,6-trimethylpyridine, 2-iminothiolane hydrochloride and solvents were purchased from Sigma-Aldrich (St Louis, MO, USA). Silica Gel 60M (230–400 mesh) was purchased from Macherey-Nagel (Duren, Germany).

Gypsum ($\text{CaSO}_4 \cdot 2\text{H}_2\text{O}$), calcite (CaCO_3) and inorganic pigments – blue smalt (potassium glass colored with cobalt(II) salts), azurite ($\text{Cu}_3(\text{CO}_3)_2(\text{OH})_2$), red ochre (Fe_2O_3), lead white ($(\text{PbCO}_3)_2 \cdot \text{Pb}(\text{OH})_2$) and minium (Pb_3O_4) employed for the preparation of paint mock-ups – were obtained from Zecchi (Firenze, Italy).

Polyester resin (Inplex) for sample embedding was purchased from Remet (Bologna, Italy). Phosphate-buffered saline (PBS) containing 10 mM phosphate, 137 mM NaCl and 2.7 mM KCl (pH 7.4) was used for the preparation of antibody solutions and for washing.

Abrasive papers for paint cross-section preparation were purchased from Micro-Surface Finishing Products Inc., Wilton, IA. All the other chemicals used were of analytical grade.

Paint samples

The standard samples employed for assessing the suitability of the immuno-localization procedures were obtained from paint mock-ups prepared in the laboratory, according to ancient painting recipes.²⁸ A gypsum ground layer was prepared with a mixture of gypsum – or gypsum and calcite – and rabbit glue (10 g dissolved in 150 mL of hot water). Then, a layer of whole-egg tempera – a mixture of egg white, yolk, and water in a 1 : 1 : 1 (v/v) ratio – was applied onto the ground layer. Additional samples were prepared with inorganic pigments and different binder mixtures. The relative ratio between paint constituents was chosen, according to their nature, to obtain homogenous mixtures suitable for application as thin layers (Table 1).

The historical sample submitted to the experimental procedure was collected from a painted wood panel by Baldassare Carrari (1460–1516), an Italian Renaissance painter, representing the Virgin with the Holy Baby and Saints and exhibited in the city museum of Ravenna, Italy (sample ROND12).

Instrumentation

Dark field observation was performed with an Olympus (Olympus Optical, Tokyo, Japan) BX51 microscope equipped with an Olympus DP70 digital scanner camera. A 100 W halogen projection lamp and an Ushio Electric (USHIO Inc, Tokyo, Japan) USH102D ultraviolet (UV) lamp were employed for the acquisition of visible and fluorescent images, respectively.

The SERS spectra were recorded with a micro-Raman Renishaw RM2000 spectrometer using a 785 nm excitation laser line. The 50× objective of a Leica microscope was used for both excitation and signal collection (180° scattering geometry). Laser power at the sample's surface was estimated to be ~1 mW. Laser beam focusing was accomplished through a 50× magnification objective that provided a 2 μm laser spot diameter. Both

Table 1 Structures of paint reconstructions

Paint reconstruction	Layers	
1L1	Layer 1 (thickness 30 μm)	Whole-egg tempera
	Layer 0 (ground layer)	Gypsum/rabbit glue
1L1b	Layer 1 (thickness 40 μm)	Animal glue
	Layer 0 (ground layer)	Gypsum/rabbit glue
1L2_a	Layer 1 (thickness 36 μm)	Lead white/egg 20 : 13 (w/w)
	Layer 0 (ground layer)	Gypsum + calcite/rabbit glue
1L2_b	Layer 1 (thickness 36 μm)	Lead white/collagen 20 : 13 (w/w)
	Layer 0 (ground layer)	Gypsum + calcite/rabbit glue
1L3	Layer 1 (thickness 50 μm)	Smalt blue/egg 4 : 1 (w/w)
	Layer 0 (ground layer)	Gypsum/rabbit glue
2L1	Layer 2 (thickness 60 μm)	Azurite/rabbit glue 5 : 2 (w/w)
	Layer 1 (thickness 13 μm)	Red ochre/egg 4 : 3 (w/w)
	Layer 0 (ground layer)	Gypsum + calcite/rabbit glue
2L2	Layer 3 (thickness 45 μm)	Lead white/egg 20 : 13 (w/w)
	Layer 1 (thickness 36 μm)	Red ochre/casein 10 : 7 (w/w)
	Layer 0 (ground layer)	Gypsum + calcite/rabbit glue

single points – randomly selected on the sample surface – and mapping analyses were performed to achieve a reliable characterization of paint components in terms of molecular spectral features and spatial identification, evaluating the selectivity of the approach for target protein recognition. The acquisition time for each spectrum was 10 s and spectra were recorded over the range 250–2000 cm^{-1} at a 1 cm^{-1} resolution. The spectrum of SERS nanotag-labelled antibody solution, as reference, was recorded from an aliquot of 1 μL deposited on a glass slide. A dedicated software program, GRAMS32, was used for a combined manipulation of the spectra dataset. Chemical mapping was performed by means of in-house Matlab routines (The Mathworks Inc., Natick, USA).

SERS probe preparation

The synthesis of AuNPs was performed by LASiS of a gold target immersed in 10^{-5} M NaCl, using 9 ns pulses of a Nd:YAG laser at 1064 nm. The laser beam was focused on the target with a fluence of 10 J cm^{-2} , allowing fast production of AuNPs with average diameters of about 20 nm.^{29,30} The synthesis of nanoparticles was monitored by extinction spectroscopy using the Mie-Gans model.²⁵ The ablation process was stopped at a AuNP concentration of 1 nM. The solution of NaCl was employed to increase the period of stability of particles up to several months. Indeed, it is known that Cl^- ions help in breaking the Au–O–Au bonds formed, during the ablation process in water, on a small part of the surface of the nanoparticles, producing Au–O[−] charges which further stabilize, by coulombic interactions, the

colloidal solution.²⁵ AuNPs are centrifuged at 30 000g for 10 minutes and suspended in water three times to obtain aggregated nanoparticles with a dimension of the order of 100 nm, as previously reported.²⁶ This dimension is needed to obtain nanostructures with a sufficient number of hot spots for a strong SERS effect. The aggregation of nanoparticles was controlled by registration of UV-Vis-NIR spectra (Fig. 1a), which showed broad extinction effects in the NIR region for aggregates characterized by larger dimensions. In fact, this latter case shows a pronounced extinction maximum at about 700–800 nm, which is important for exciting the localized plasmon resonance of the nanoparticles in the NIR, according to the excitation wavelength.

Reaction of Nile Blue A perchlorate and lipoic acid was obtained in DMF solution in the presence of HATU and 2,4,6-trimethylpyridine. The solution was stirred overnight at room temperature, then the solvent was evaporated and the product was purified by normal phase liquid chromatography (eluent CH₃OH 10% in CHCl₃). The product was characterized by ESI-TOF mass spectrometry (506,19 *m/z* for lipoic acid functionalized Nile Blue).

The SERS reporter was linked to the aggregated nanoparticles by mixing a colloidal solution of the nanoparticles with that of the reporter. The S–S group of the lipoic acid allowed fast binding of molecules to AuNPs. Afterwards, the antibody was functionalized with one thiol group, on average, with 2-iminothiolane, as previously reported²⁵ and then linked to the aggregated AuNPs already functionalized with LipNB. The solution was then purified by centrifugation and dispersed in

PBS. The amount of antibody bound to the nanoparticles was evaluated on the basis of the absorption of the supernatant after the conjugation with the nanostructures. The rough average estimate shows that up to a few tens (10–20) of antibodies can be present on a nanoparticle, although this estimation can depend on the aggregation of nanoparticles. Finally, nanostructures were treated with thiolated polyethylene glycol chains (5000 MW, 0.5 mg mL^{−1}), in order to completely coat the free surface of the aggregated nanoparticles with a layer of a protecting polymer. This allows non-specific interactions to be avoided or minimized, without compromising the highly selective interaction between antibody and antigen. The main steps of the SERS probe preparation are reported in Fig. 1b.

Immunoassay

Cross-sections were prepared according to previously reported standard procedures.³¹ Briefly, the micro-samples (with size of a few square millimeters) obtained from the mock-ups were embedded in polyester resin and polished with silica abrasive papers (grit from 120 to 1000) and water as a cooling medium. Then, to obtain a high-quality surface in terms of planarity and roughness, a dry polishing procedure was performed using SiC papers graded from 2400 up to 12 000.

A non-competitive sandwich-type immunoassay with SERS mapping detection was applied to spatially locate the ovalbumin in paint samples. Cross-sections were treated for 20 minutes at room temperature with the non-specific blocking

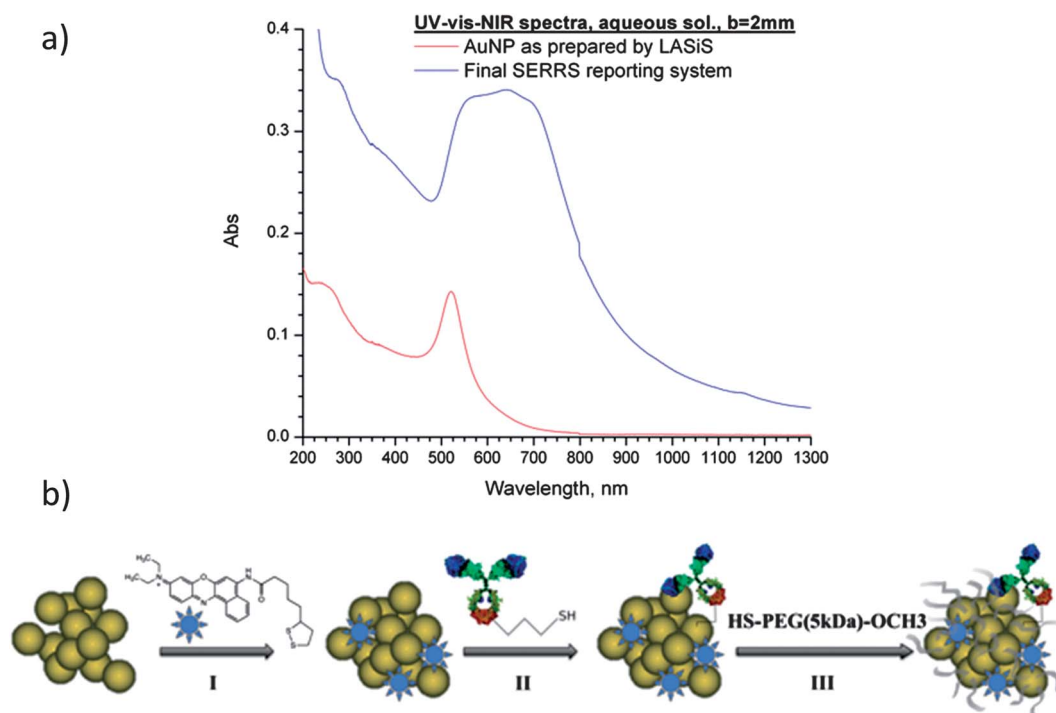


Fig. 1 (a) Extinction spectra of the non-aggregated AuNPs (red line), and aggregated AuNPs after the functionalization with the Nile Blue and the secondary antibody (blue line); (b) steps for the preparation of the SERS probes: (I) aggregated nanoparticles obtained by centrifugation linked with the Nile Blue reporter; (II) functionalization of the secondary antibody to the nanoaggregate; (III) covering of the nanoaggregate with thiolated polyethylene glycol chains.

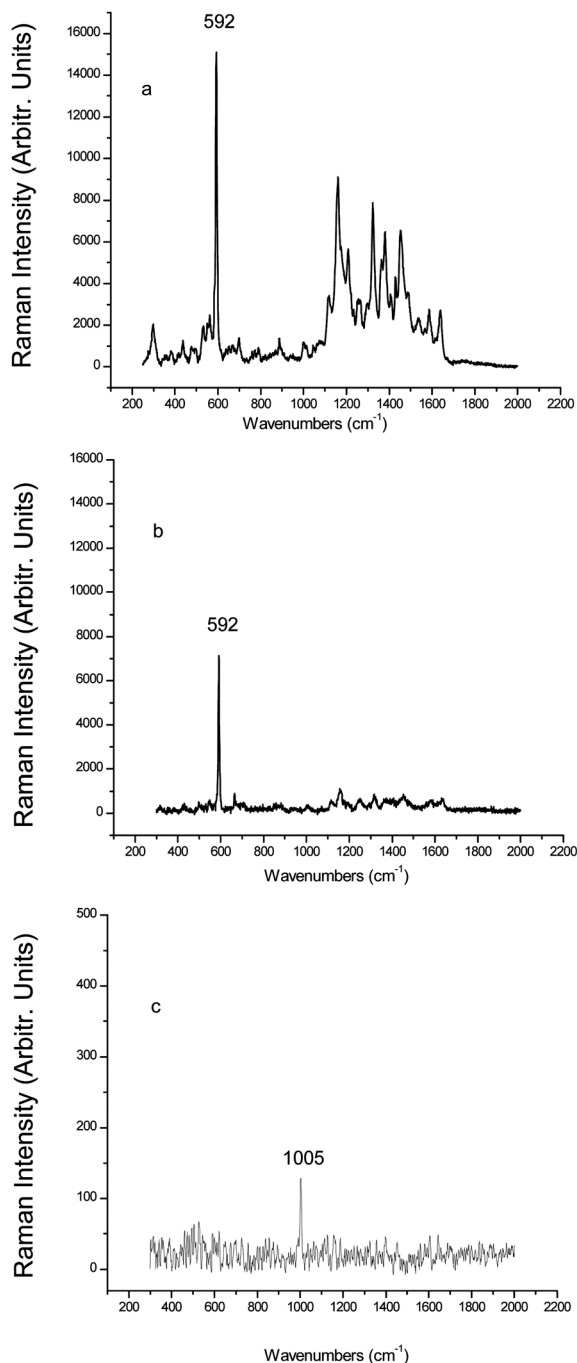


Fig. 2 Raman spectra of (a) SERS nanotag-labeled secondary antibody; (b) spectrum collected from the whole egg-tempera layer of sample 1L1; (c) spectrum collected from the preparation layer.

solution (1% dried milk in water) and washed with PBS. Subsequently, the cross-sections were incubated with the anti-chicken egg albumin antibody (primary antibody) diluted 3 : 100 (v/v) in PBS. Afterwards, the samples were washed three times with PBS and incubated for 4 h at 37 °C with the SERS nanotag-labeled anti-rabbit IgG antibody (secondary antibody) diluted 1 : 100 (v/v) in PBS. Samples were washed again three times with PBS. After air-drying, treated cross-sections were analyzed by Raman microscopy.

Results and discussion

Optimization of experimental conditions

Preliminary investigations on the efficiency of the proposed approach were carried out on standard samples collected from paint reconstructions, which were obtained by application of a single layer of whole-egg tempera onto the gypsum ground layer (sample 1L1). According to previous research work aimed at the localization of ovalbumin,^{5,31} dried non-fat bovine milk was employed as a blocking agent in immunoassays to avoid non-specific adsorption of immuno-reagents and non-specific interactions between antibodies and paint components in layers which do not contain the target protein. This step plays a crucial role in defining suitable immunoassay experimental conditions, especially for the detection of an analyte present in porous and heterogeneous samples. Moreover, it is worth mentioning that water-soluble components (such as gypsum) may increase the non-specific binding of the reagents. In fact, the preparation layer made with gypsum and animal glue can easily interact with reagents during the incubation steps, due to its chemical and physical nature. Nevertheless, such a layer should not present any signal ascribable to the SERS reporter because it does not contain the target protein (ovalbumin). Indeed, an appropriate blocking solution and incubation conditions for antibodies were carefully selected, to reduce the non-specific SERS reporter signal. Particular attention was also paid to the preparation of cross-sections, applying a dry polishing procedure to improve the sample surface quality and homogeneity.³¹ In an attempt to promote the specific interaction between primary antibody and SERS-nanotags labelled secondary antibody, incubations of the secondary antibody were performed under thermostatic conditions.

The analysis allowed the clear localization of ovalbumin within the whole-egg tempera layer, thanks to the identification of the Nile blue marker band at 592 cm^{-1} (Fig. 2b), which is the most intense peak in the SERS-reporter spectrum obtained with the excitation line at 785 nm. Moreover, peaks detectable in the region between 1000 and 1800 cm^{-1} , which are clearly visible in the spectrum of the labelled secondary antibody, reported in Fig. 2a as the reference, can be also ascribable to the presence of the SERS nanotags. Several measurement points were investigated for different paint sample replicas to verify the reproducibility of the results and the selectivity of the method. As expected, analyses performed on the ground layer, composed of gypsum and animal glue, permitted the identification of gypsum, while any peak ascribable to the presence of the SERS probe was identified (Fig. 2c).

For a deeper evaluation of the performances of the proposed approach, the immunoassay was applied on different types of paint reconstructions, characterized by different stratigraphies and components.

It is important to underline that all the observed bands were identified due to normal Raman spectra and only those of Nile Blue were related to the SERS effect.

In particular, samples presenting a single pigment layer – containing lead white (sample 1L2a) or blue smalt (sample 1L3) mixed with whole egg tempera – were investigated. As expected,

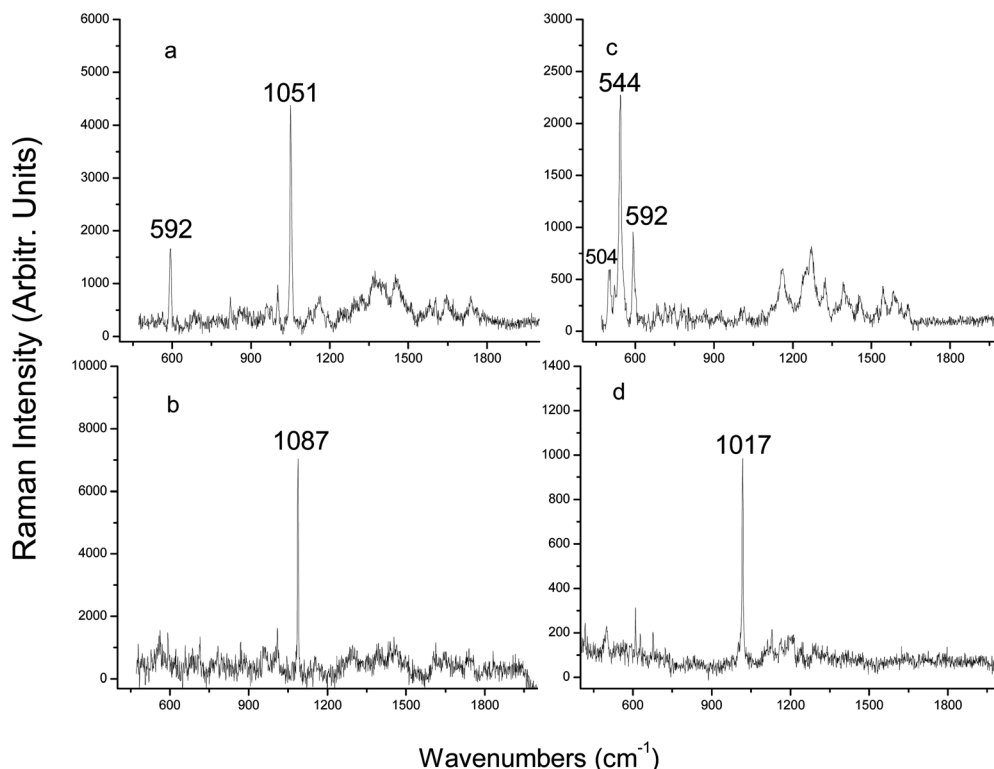


Fig. 3 (a) Raman spectrum collected from the white pigment layer of sample 1L2a; (b) Raman spectrum collected from the preparation layer of sample 1L2a; (c) Raman spectrum collected from the blue pigment layer of sample 1L3; (d) Raman spectrum collected from the preparation layer of sample 1L3.

it was possible to determine the presence of lead white and ovalbumin in the pigment layer 1 in sample 1L2a, thanks to the peaks at 1051 cm^{-1} (related to the symmetric CO_3^{2-} stretching mode) and at 592 cm^{-1} (related to the SERRS reporter band), respectively (Fig. 3a). Moreover, the SERS reporter bands were also identified in the blue pigment layer 1 of sample 1L3 (Fig. 3c).

Interestingly, in this blue sample it was possible to reveal the presence of cobalt blue ($\text{CoO} \cdot \text{Al}_2\text{O}_3$), thanks to the peak at 504 cm^{-1} . In addition, an artificial ultramarine was also identified (S_3^- stretching mode at 544 cm^{-1}), pointing out the real composition of the pigment, commercially available as blue smalt. Finally, it was possible to recognize in the ground layer the presence of calcite in sample 1L2a (peak at 1087 cm^{-1} of the symmetric CO_3^{2-} stretching) and gypsum in sample 1L3 (peak at 1017 cm^{-1} of the symmetric SO_4^{2-} stretching). Also, in these cases, no contribution from the SERS reporter was detected in layers without ovalbumin (Fig. 3b and d).

Assay selectivity

The evaluation of performances in terms of assay selectivity was carefully taken into account to compare the results with those reported in the literature.⁸ Indeed, problems related to the inability of removing SERS nanotags non-specifically bonded, producing false positive signals and seriously compromising the effectiveness of the analytical response, were indicated as the major drawback of the method.

First the immuno-localization of ovalbumin was performed in standard sample replicas with a pigment layer containing lead white and egg-tempera (sample 1L2a) without the primary antibody. In such a case, even if the analyte (ovalbumin) is present in the pigment layer, no SERS reporter signal should be detected due to the absence of the primary antibody, as observed in the results obtained (Fig. 4a), which showed uniquely the presence of lead white due to the Raman peak at 1051 cm^{-1} . Moreover, analysis on this sample allowed the

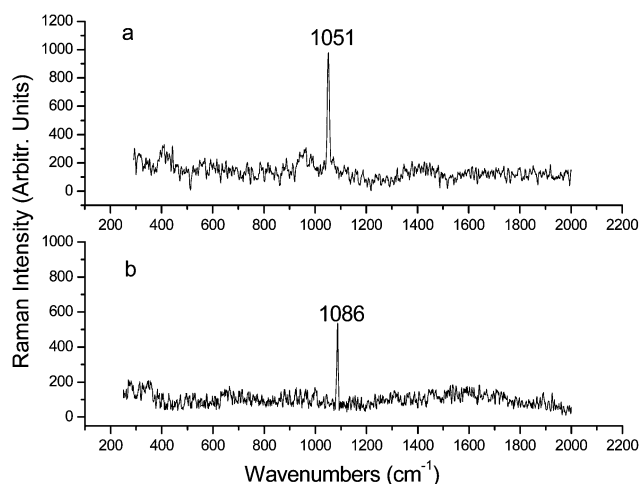


Fig. 4 Sample 1L2a: (a) Raman spectrum collected from the white pigment layer; (b) Raman spectrum collected from the preparation layer.

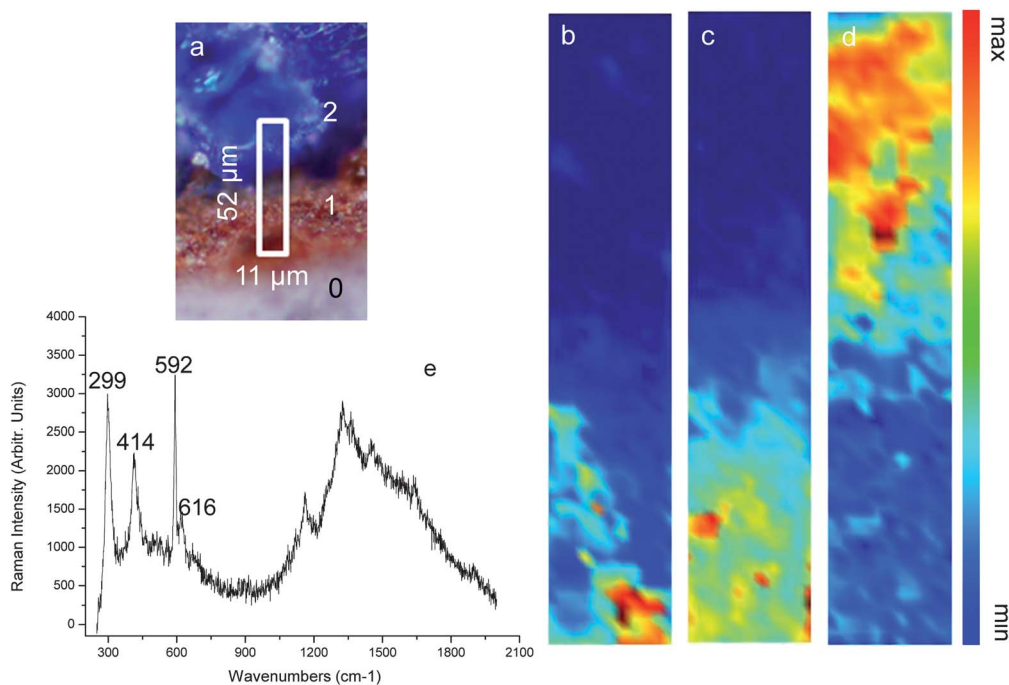


Fig. 5 (a) Cross-sectional microphotograph of sample 2L1 under visible light. The white box indicates the selected area for Raman analysis. Chemical false colour maps of (b) Nile Blue (band at 592 cm^{-1}); (c) red ochre (band at 299 cm^{-1}); (d) azurite (band at 400 cm^{-1}); (e) spectrum extracted from layer 1.

verification of the absence of any non-specific signals also from the preparation layer, where it was possible to identify the presence of calcium carbonate thanks to the band at 1086 cm^{-1} (Fig. 4b). Afterwards, paint stratigraphies characterized by the presence of a different type of protein (collagen) either with or

without the pigment (sample 1L1b and 1L2b) were submitted to the complete immunoassay. Also in these cases, Raman measurements carried out for the treated paint stratigraphies showed the complete absence of the SERS reporter diagnostic band, both in the pigment and in the ground layer. Such results

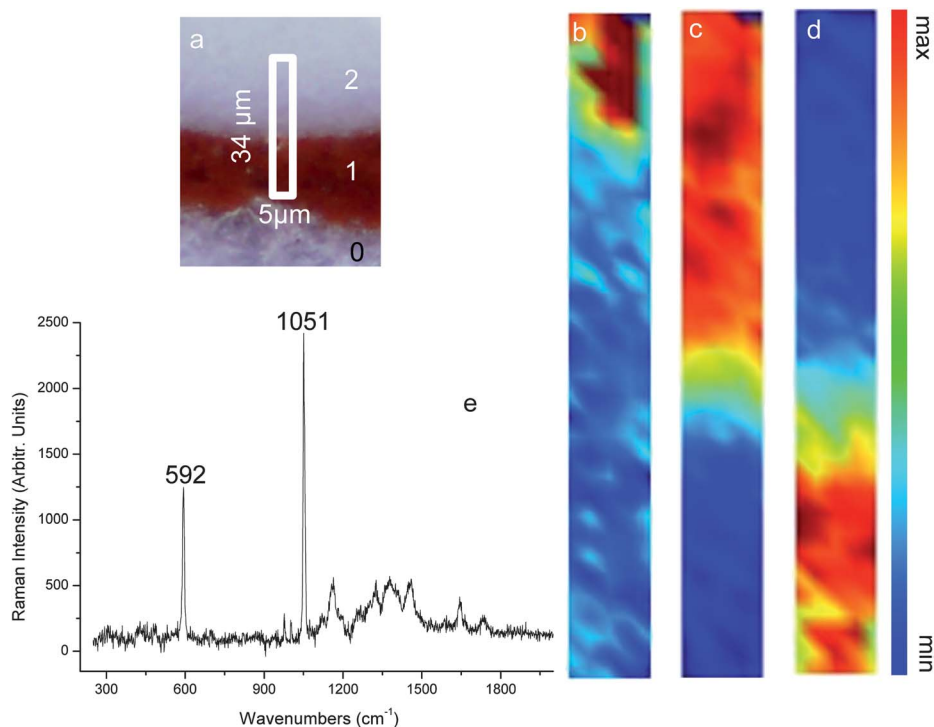


Fig. 6 (a) Cross-sectional microphotograph of sample 2L2 under visible light. The white box indicates the selected area for Raman analysis. Chemical false colour maps of (b) Nile Blue (band at 592 cm^{-1}); (c) red ochre (band at 299 cm^{-1}); (d) lead white (band at 1051 cm^{-1}); (e) spectrum extracted from layer 2.

confirmed that blocking and washing steps, as well as incubation times, were correctly set up.

Mapping analysis on standard and historical samples

After the optimization of the indirect SERS immunoassay procedure, more complex paint stratigraphies were investigated. In particular, standard samples presenting two pigment layers containing different proteins and pigments (samples 2L1 and 2L2) were submitted for SERS analysis. Sample 2L1 was mapped using a step of $1\ \mu\text{m}$ in the x - y direction, over an area of $52 \times 11\ \mu\text{m}^2$, with 572 spectra recorded. An area of $34 \times 5\ \mu\text{m}^2$ was investigated in sample 2L2, using a step of $1\ \mu\text{m}$ in the x - y direction and acquiring 170 spectra. In order to achieve a representative distribution of components, chemical maps were re-constructed, selecting the diagnostic Raman band for a given compound and, simultaneously, it was possible to exactly localize ovalbumin, thanks to the selection of the Nile Blue SERRS band. In particular, the presence of ovalbumin and red ochre was detected in layer 1 of sample 2L1 by integration of bands at $592\ \text{cm}^{-1}$ and $299\ \text{cm}^{-1}$, respectively (Fig. 5b and c). Moreover, lead white and egg tempera were visualized in layer 2 of sample 2L2 by re-construction of chemical maps using the band at $1051\ \text{cm}^{-1}$ for the localization of lead white and the band at $592\ \text{cm}^{-1}$ for the detection of ovalbumin (Fig. 6b and c). An intense Raman reporter signal was clearly located in the

upper part of layer 2, probably due to a higher concentration of binder in this area, even if the presence of the marker band was recognized all over the lead white layer.

In contrast, non-specific SERRS reporter signals were not identified in layers containing a different proteinaceous material used as binding medium (such as rabbit glue in layer 2 of sample 2L1 and casein layer 1 of sample 2L2). The identification of diagnostic bands at 400 and $299\ \text{cm}^{-1}$ (used for the reconstruction of chemical maps), assigned to Cu-O stretching modes and E_g hematite vibrational modes,³² respectively, allowed the localization of azurite (layer 2, Fig. 5d) and red ochre (layer 1 Fig. 6d). Moreover, it was also possible to verify the presence of gypsum and calcium carbonate in the ground layer.

Finally, the proposed method was tested on a historical sample, collected from a Renaissance painting. Mapping analysis was performed on an area of $19 \times 3\ \mu\text{m}^2$, using a step of $1\ \mu\text{m}$ in the x - y direction. A total of 57 spectra were acquired. The immunochemical detection of ovalbumin performed by Raman SERS allowed the characterization of the varnish layer, thanks to the unambiguous localization of Nile Blue spectral features within the uppermost layer of the stratigraphy, identifying the diagnostic band at $592\ \text{cm}^{-1}$ (Fig. 7b). In particular, in the spectrum extracted from the related area of the map (Fig. 7f) it was possible to recognize the spectral features of the SERS reporter and two weak bands at 1000 and $1039\ \text{cm}^{-1}$, which may be ascribable to the contamination of the

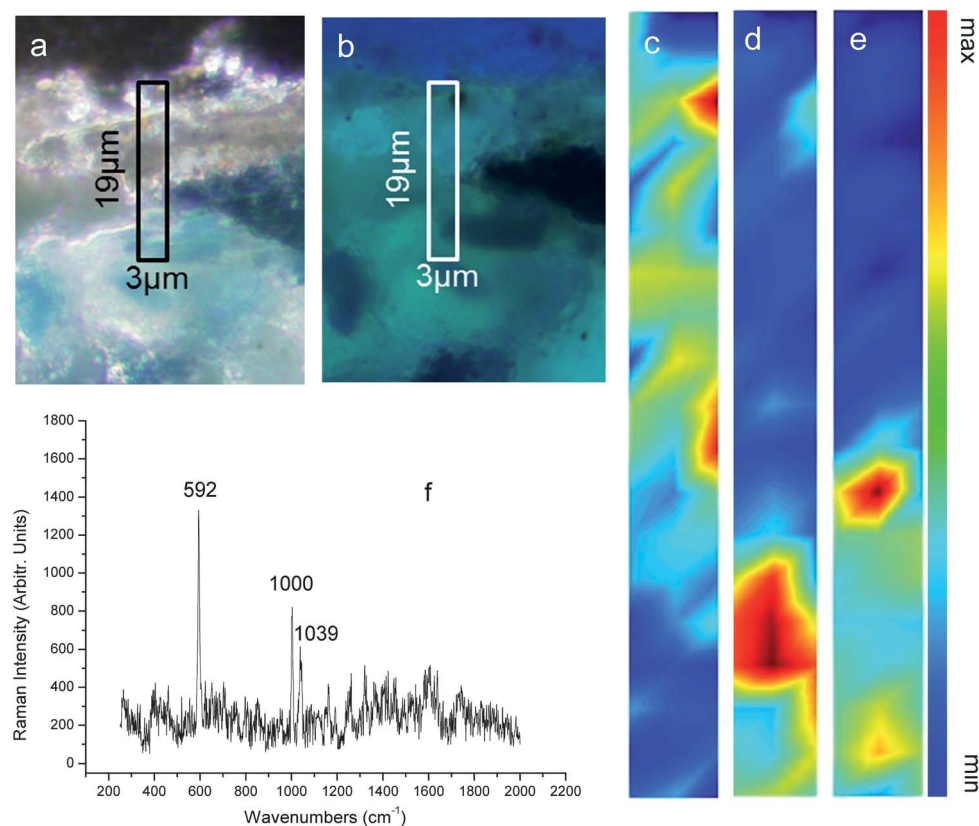


Fig. 7 Cross-sectional microphotographs of sample ROND12: (a) image under visible light; (b) image under UV illumination. Black and white boxes indicate the selected area for Raman analysis. Chemical false colour maps of (c) Nile Blue (band at $592\ \text{cm}^{-1}$); (d) azurite (band at $400\ \text{cm}^{-1}$); (e) lead white (band at $1051\ \text{cm}^{-1}$); (f) spectrum extracted from the varnish layer.

embedding resin.³³ This result is in agreement with the previous analyses performed by chemiluminescent immunochemical identification, which allowed the localization of a thin external layer of ovalbumin,^{5,31} probably applied as the finishing layer. Also in this case, the immuno-SERS analysis, combined with the traditional Raman spectroscopy, provided information on the composition of the other layers. In more detail, it was possible to localize the presence of azurite mixed with lead white within the pigment layer, by identifying the Cu–O stretching band at 400 cm^{−1} for the location of azurite and the band related to the symmetric CO₃^{2−} stretching at 1051 cm^{−1} for the localization of lead white (Fig. 7c and d).

Conclusion

The developed SERS immunolocalization procedure combined the selectivity of immunological reactions with the high sensitivity of the SERS technique, with the advantage of obtaining Raman information of the other components present in the sample. Mapping analyses performed on both standard mock-ups and on a real sample showed the optimal performance of the method for the selective location of ovalbumin and of the other Raman active components present inside the paint stratigraphy. With respect to the other published immunological methods based on chemiluminescence and fluorescence detection, the proposed approach allows us to obtain the maximum information from the same specimen, reducing the number of samples to be collected and of techniques to be employed.

The paper proposed the use of alternative SERS probes obtained by LASiS as a marker of the secondary antibody. This method is an excellent green and cheap alternative to the traditional chemical nanoparticles synthesis, providing a highly efficient detection of the target protein both in fresh and historical samples.

The immunological protocol was developed in order to overcome drawbacks recently reported in the literature related to the presence of non-specific signals. In particular, blocking and washing steps as well as incubation times were optimised.

Future perspectives will foresee the optimisation of multiplexed immunolocalization assays for the simultaneous and selective localization of different proteinaceous components. This will be achieved using different analyte-specific primary antibodies detectable by species-specific secondary antibodies labelled with different Raman reporters.

Acknowledgements

The present work was carried out with the support of Italian Ministry for University and Research (MIUR) (PRIN08) and the 7^o FP (CHARISMA-Cultural Heritage Advanced Research Infrastructures: Synergy for a Multidisciplinary Approach to Conservation/Restoration Project no. 228330).

References

- 1 D. Wild, *The immunoassay handbook*, Elsevier, Amsterdam, 3rd edn, 2005.
- 2 B. Ramirez Barat and S. de la Vina, *Stud. Conserv.*, 2001, **46**, 282–288.
- 3 A. Heginbotham, V. Millay and M. Quick, *J. Am. Inst. Conserv.*, 2006, **45**, 89–105.
- 4 G. Sciutto, L. S. Dolci, A. Buragina, S. Prati, M. Guardigli, R. Mazzeo and A. Roda, *Anal. Bioanal. Chem.*, 2011, **399**, 2889–2897.
- 5 G. Sciutto, L. S. Dolci, M. Guardigli, M. Zangheri, S. Prati, R. Mazzeo and A. Roda, *Anal. Bioanal. Chem.*, 2013, **405**, 933–940.
- 6 L. Cartechini, M. Vagnini, M. Palmieri, L. Pitzurra, T. Mello, J. Mazurek and G. Chiari, *Acc. Chem. Res.*, 2010, **43**, 867–876.
- 7 I. Sandu, S. Schäfer, D. Magrini, S. Bracci and C. Roque, *Microsc. Microanal.*, 2012, **18**, 860–875.
- 8 J. Arslanoglu, S. Zaleski and J. Loike, *Anal. Bioanal. Chem.*, 2011, **399**, 2997–3010.
- 9 S. Nie and S. R. Emory, *Science*, 1997, **275**, 1102–1106.
- 10 R. Aroca, *Surface-Enhanced Vibrational Spectroscopy*, John Wiley & Sons, West Sussex, 2006.
- 11 E. C. Le Ru and P. G. Etchegoin, *Principles of Surface Enhanced Raman Spectroscopy and related plasmonic effects*, Elsevier, Amsterdam, 2009.
- 12 S. L. Kleinman, R. R. Frontiera, A. I. Henry, J. A. Dieringer and R. P. Van Duyne, *Phys. Chem. Chem. Phys.*, 2013, **15**, 21–36.
- 13 J. P. Camden, J. A. Dieringer, Y. Wang, D. J. Masiello, L. D. Marks, G. C. Schatz and R. P. Van Duyne, *J. Am. Chem. Soc.*, 2008, **130**, 12616–12617.
- 14 A.-I. Henry, J. M. Bingham, E. Ringe, L. D. Marks, G. C. Schatz and R. P. Van Duyne, *J. Phys. Chem.*, 2011, **115**, 9291–9305.
- 15 V. Amendola and M. Meneghetti, *Adv. Funct. Mater.*, 2012, **22**, 353–360.
- 16 B. R. Lutz, C. E. Dentinger, L. N. Nguyen, L. Sun, J. Zhang, A. N. Allen, S. Chan and B. S. Knudsen, *ACS Nano*, 2008, **2**, 2306–2314.
- 17 B. R. Lutz, C. E. Dentinger, L. Sun, L. Nguyen, J. Zhang, A. J. Chmura, A. Allen, S. Chan and B. Knudsen, *J. Histochem. Cytochem.*, 2008, **56**, 371–379.
- 18 D. S. Grubisha, R. J. Lipert, H. Y. Park, J. Driskell and M. D. Porter, *Anal. Chem.*, 2003, **75**, 5936–5943.
- 19 X. Su, J. Zhang, L. Sun, T. W. Koo, S. Chan, N. Sundararajan, M. Yamakawa and A. A. Berlin, *Nano Lett.*, 2005, **5**, 49–54.
- 20 C. Lofrumento, M. Ricci, E. Platania, M. Becucci and E. Castellucci, *J. Raman Spectrosc.*, 2013, **44**, 47–54.
- 21 M. Leona, P. Decuzzi, T. A. Kubic, G. Gates and J. R. Lombardi, *Anal. Chem.*, 2011, **83**, 3990–3993.
- 22 S. Murcia-Mascarós, C. Domingo, S. Sanchez-Cortes, M. V. Cañamares and J. V. Garcia-Ramos, *J. Raman Spectrosc.*, 2005, **36**, 420–426.
- 23 B. Doherty, B. G. Brunetti, A. Sgamellotti and C. Miliani, *J. Raman Spectrosc.*, 2011, **42**, 1932–1938.
- 24 F. Casadio, M. Leona, J. R. Lombardi and R. Van Duyne, *Acc. Chem. Res.*, 2010, **43**, 782–791.
- 25 V. Amendola and M. Meneghetti, *J. Phys. Chem.*, 2009, **113**, 4277–4285.

- 26 M. Meneghetti, A. Scarsi, L. Litti, G. Marcolongo, V. Amendola, M. Gobbo, M. Di Chio, A. Boscaini, G. Fracasso and M. Colombatti, *Small*, 2012, **8**, 3733–3738.
- 27 D. Hazafy, M. V. Salvia, A. Mills, M. G. Hutchings, M. P. Evstigneev and J. A. Parkinson, *Dyes Pigm.*, 2011, **88**, 315–325.
- 28 C. Cennini and F. Frezzato, *Il libro dell'arte*, ed. Neri Pozza, Milano, 2004.
- 29 V. Amendola and M. Meneghetti, *J. Mater. Chem.*, 2007, **17**, 4705–4710.
- 30 V. Amendola, S. Polizzi and M. Meneghetti, *J. Phys. Chem. B*, 2006, **110**, 7232–7237.
- 31 L. S. Dolci, G. Sciutto, M. Guardigli, M. Rizzoli, S. Prati, R. Mazzeo and A. Roda, *Anal. Bioanal. Chem.*, 2008, **392**, 29–35.
- 32 A. Zoppi, C. Lofrumento, E. M. Castellucci and P. Sciau, *J. Raman Spectrosc.*, 2008, **39**, 40–46.
- 33 A. H. Kuptsov, *J. Forensic Sci.*, 1994, **39**, 305–318.